Chain of Thought in Order: Discovering Learning-Friendly Orders for Arithmetic

Yuta Sato [1] Kazuhiko Kawamoto [1] Hiroshi Kera [1 2]

Abstract

The chain of thought is fundamental in Transformers, which is to perform step-by-step reasoning. Besides what intermediate steps work, the order of these steps critically affects the difficulty of the reasoning. This study addresses a novel task of unraveling chain of thought—reordering decoder input tokens to a learning-friendly sequence for Transformers to learn arithmetic tasks. The proposed pipeline first trains a Transformer on a mixture of target sequences arranged in different orders and then identifies benign orders as those with fast loss drops in the early stage. As the search space grows factorially with sequence length, we propose a two-stage hierarchical approach for inter- and intra-block reordering. Experiments on four order-sensitive arithmetic tasks show that our method identifies a learning-friendly order out of a few billion candidates. Notably, on the multiplication task, it recovered the reverse-digit order reported in prior studies.

1. Introduction

Autoregressive generation is central to the success of the Transformer (Vaswani et al., 2017) in reasoning tasks, which leads to many successes of the end-to-end learning of arithmetic and hard symbolic computations, such as (Lample & Charton, 2020; Charton, 2022; Kera et al., 2024; 2025; Alfarano et al., 2024; Wenger et al., 2022; Li et al., 2023a;b). The autoregressive nature makes each reasoning step conditioned on the preceding context, and careful design of intermediate reasoning steps, such as *chain of thought* (Wei et al., 2022), guides the model's reasoning toward the final answer of the target problem. For example, it has been known that learning the parity function—the prediction of the parity of the input bit string—is challenging (Shalev-Shwartz et al., 2017; Hahn & Rofin, 2024). However, Kim & Suzuki (2025) recently has shown that the step-by-step prediction of the parity of the first k bits with $k = 1, 2, \ldots$, makes the learning successful.

One important yet underexplored aspect is the order of the chain of thought—not only which steps to include, but also the *order* in which they are arranged can greatly impact learning. For example, Shen et al. (2023) has shown that the Transformer learns multiplication of two integers with better generalization to larger integers (i.e., those with more digits) when the product is generated from least to most significant digits (cf. Figure 1). While this particular case can be explained by the carries, which flow from least to most significant digits, a systematic way of determining a learning friendly order of the chain of thought remains unknown.

In this study, we address a new task of reordering decoder input tokens, or *unraveling* chain of thought presented in an unfriendly order, for better reasoning, particularly in arithmetic tasks. Exploiting the observation that neural networks tend to learn from easy to hard instances during training (Arpit et al., 2017; Forouzesh & Thiran, 2024; Swayamdipta et al., 2020), we train a Transformer on a mixture of target sequences in different orders and identify those that lead to a faster loss drop in the early stages of training. To better handle longer sequences, we propose a two-stage hierarchical approach, where the global stage finds block-level orders, while the local stage reorders tokens within each block.

The experiments demonstrate that the proposed method successfully reorders the target sequences. We designed three arithmetic tasks that are relatively easy to compute with the (input and) target sequence in the forward order but not with other orders. Starting from random orders, the proposed method succeeds up to thirteen tokens (i.e., $13! > 6 \times 10^9$ permutations), increasing the success rate of arithmetic computation from approximately 10 % to 100 %. We also applied our method to the multiplication task in (Shen et al., 2023) and successfully rediscovered the reverse orders.

Our contributions are summarized as follows:

- We address a novel task of unraveling chain of thought

[*] Equal contribution [1] Chiba University [2] Zuse Institute Berlin. Correspondence to: Hiroshi Kera <kera@chiba-u.jp>.

The second AI for MATH Workshop at the 42^{nd} International Conference on Machine Learning, Vancouver, Canada.

to reorder the target tokens so that the learning becomes more successful for in-distribution samples and generalizable to out-distribution samples.

- We propose a method that efficiently determines learning-friendly orders from the loss profile at the early stage of training. Empirically, this filters a few thousand candidates in a single epoch, and combined with a hierarchical strategy, the best order can be found out of a few billion candidates.

- We introduce order-sensitive arithmetic tasks using non-injective maps and present extensive experiments, where the proposed method is evaluated when starting with random permutations and partially sorted ones. Not only on the proposed tasks but also recovered the previously reported orders in the multiplication task.

2. Related work

Transformers for mathematical tasks. Transformers have recently been applied to mathematical problem-solving with encouraging results. (Lample & Charton, 2020) has demonstrated that a Transformer can carry out integral calculus with a high success rate, opening the possibility that sequence-to-sequence models can handle algebraic tasks. Since that study, applications have expanded to arithmetic (Charton, 2022), linear algebra (Charton, 2022), computational algebra (Kera et al., 2024; 2025), and coding theory as well as cryptography (Wenger et al., 2022; Li et al., 2023a;b). One reason behind these successes is the autoregressive generation scheme. Although theory has suggested that learning high-sensitive functions such as parity is difficult (Hahn & Rofin, 2024), recent work achieved a high success rate on parity tasks by applying chain of thought prompting (Wei et al., 2022; Kojima et al., 2022; Chen et al., 2023; Yao et al., 2023; Zhang et al., 2024) to arithmetic and by exploiting the generated output tokens effectively (Kim & Suzuki, 2025). Positional encoding is also crucial for arithmetic problems; prior work (Jelassi et al., 2023) has shown that relative-position and abacus-style embeddings improve generalization to out-of-distribution data. These studies collectively show that task-specific representations and positional encodings strongly influence performance. In particular, prior work (Shen et al., 2023) analyzed in detail how digit order affects multiplication success rate and demonstrated that generating digits from the least significant position upward raises the success rate; however, the ordering was chosen heuristically rather than by an automated procedure. Systematic optimization of the output order itself in arithmetic tasks remains unaddressed. This study is the first to exploratively optimize the output-sequence *permutation* for each task, automatically discovering a learning-friendly target order.

Training tendencies of DNNs. The observation that DNNs can be trained even on randomly assigned labels—while still achieving excellent generalization on real data—led to a line of research into how models adapt to data during training (Zhang et al., 2017). (Arpit et al., 2017) has experimentally shown that networks first pick up simple regularities between inputs and labels and only later transition to memorizing harder, noise-like examples. More broadly, DNNs are known to learn easy instances in a dataset before gradually fitting the more difficult ones; in image domains, this behavior is often referred to as spectral bias (Rahaman et al., 2019). This property is now widely exploited in curriculum learning (Jiang et al., 2018; Han et al., 2018; Baldock et al., 2021) and data-quality control (Swayamdipta et al., 2020). For example, integrating each sample's learning curve can reveal mislabeled data (Forouzesh & Thiran, 2024). Most prior work, however, analyzes such dynamics by injecting noise directly into the target labels themselves. In contrast, this study focuses on the ordering of the target sequences. The dataset is rearranged with multiple permutation matrices, and the model is trained on these reordered versions to investigate how sequence order affects learning.

3. Unraveling Chain-of-Thought

Let S_L be the symmetric group of order L, i.e., the set of all permutations over $\{1, \dots, L\}$. We address a problem of discovering a permutation $\pi \in S_L$ over the token sequence (of length L) to the Transformer decoder that improves the overall learning effectiveness of the Transformer.

The Transformer decoder generates output sequences in an auto-regressive manner. It is widely known—especially in the context of chain-of-thought prompting—that the order of generation can have a crucial impact on the reasoning ability of Transformers. For example, Figure 1 shows that, in the task of multiplying two integers, the digits of the target integer (each treated as a token) should be presented in reverse order—from lower to higher digits—because this allows the Transformer to compute carries step by step.

More generally, for example, let $X = [x_1, \dots, x_L]$ be a sequence of numbers, which is the input sequence to the Transformer. If the target sequence is defined by a map $f(x, y)$ that is non-injective with respect to y (e.g., $f(x, y) = \max\{x + y, 0\}$) as $Y = [y_1, \dots, y_L]$ with $y_1 = x_1$ and $y_{i+1} = f(x_i + y_i)$ for $i > 1$, learning from reverse order $Y^{\mathrm{r}} = [y_L, \dots, y_1]$ is significantly harder than that from the forward order because of non-injective $f(x, y)$.

We now introduce our formal problem setup as well as its challenges.

Formulation. Let Σ be the set of all tokens. We denote the set of all finite token sequences by Σ^* and its restriction

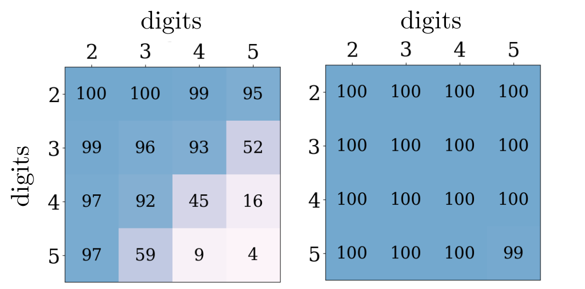

digits	2	3	4	5
2	100	100	99	95
3	99	96	93	52
4	97	92	45	16
5	97	59	9	4

(a) most-significant-digit order

digits	2	3	4	5
2	100	100	100	100
3	100	100	100	100
4	100	100	100	100
5	100	100	100	99

(b) least-significant-digit order

Figure 1. Success rates for the multiplication of two integers. Matrix rows and columns indicate the number of digits in each operand. Evaluation is conducted with 100 samples for each digit position. (a) Model trained with the standard (forward) order. (b) Model trained with the reverse order.

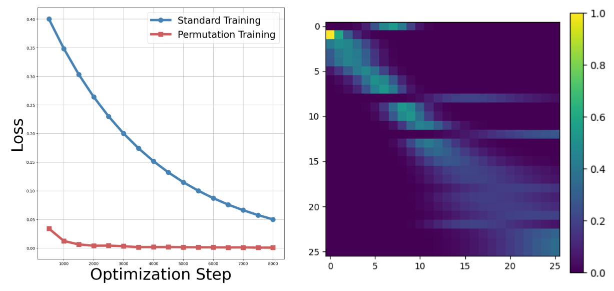

(a) Eval loss curve (b) Optimized Permutation

Figure 2. (a) Training-loss curves for a vanilla Transformer (blue) and for a model trained with soft-permutation optimization (red). The permutation-trained model's loss drops rapidly, far more steeply than in standard training. (b) Permutation matrix learned during permutation training. Sparse off-diagonal weights clustered around the main diagonal indicate leakage from future tokens.

to length-L sequences by Σ^L. Let $\mathcal{T}_\theta : \Sigma^* \times \Sigma^L \to \Sigma^L$ be a Transformer with parameter θ. Hereinafter, we assume that the target sequence length is fixed. Now, let $(X, Y) \sim \mathcal{D}$ be an input–target sequence pair (X, Y) with $|Y| = L$ from a joint distribution $\mathcal{D}$. The empirical risk minimizer (ERM) θ_{ERM} with finite sample set $D = \{(X_i, Y_i)\}_{i=1}^m$ and permutation $\pi \in S_L$ is

$$\theta^{\pi}_{\mathrm{ERM}} = \arg\min_{\theta} \frac{1}{m} \sum_{i=1}^{m} \ell(\mathcal{T}_\theta, X_i, \pi(Y_i)), \tag{3.1}$$

with ℓ denotes a loss function. Our goal is to discover a permutation π that minimizes the expected risk:

$$\pi^* = \arg\min_{\pi \in S_L} \mathbb{E}_{(X,Y)\sim\mathcal{D}}\left[\ell\left(\mathcal{T}_{\theta^{\pi}_{\mathrm{ERM}}}, X, \pi(Y)\right)\right]. \tag{3.2}$$

A permutation $\pi(Y)$ of a target sequence $Y = [y_1, \ldots, y_L] \in \Sigma^L$ can be represented as a matrix product YP, where $P \in \{0,1\}^{L\times L}$ is a permutation matrix.

Challenges. The optimization over permutations is challenging because one has to test all possible permutations, the number of which is $L!$ for those over $\{1, \ldots, L\}$. One may introduce a soft permutation matrix $\tilde{P} \in [0,1]^{L\times L}$ and perform empirical risk minimization jointly over θ and $\tilde{P}$; namely,

$$\min_{\theta, \tilde{P}} \frac{1}{m} \sum_{i=1}^{m} \ell(\mathcal{T}_\theta, X_i, Y_i\tilde{P}). \tag{3.3}$$

However, as shown in Figure 2, such an approach leads to an immediate loss drop at the early stage of training, because the soft permutation $\tilde{P}$ causes information leakage from future tokens; each token in Y_iP is a soft mixture of all the tokens in Y, which undermines the next-token prediction. Introducing an additional loss that strongly penalizes non-dominant entries in $\tilde{P}$ and encourages it to approximate a hard permutation matrix P can mitigate such leakage. However, training over nearly hard permutation matrices induces a highly non-convex loss surface, and the optimization process is prone to getting trapped in local minima (Mena et al., 2018; Jang et al., 2017).

Analysis of attention sparsity. To address the challenges of permutation optimization, we undertake a more detailed analysis. Intuitively, when the target order is learning-friendly, the causal structure of the sequence is broken: more input and output tokens become relevant to predicting the next token. Conversely, for an learning-friendly order we expect the attention map to be *sparser*.

Let the query and key matrices be $Q, K \in \mathbb{R}^{L' \times d_{\mathrm{emb}}}$, where L' is the decoder-input length and d_{emb} the embedding dimension. The self-attention weights are

$$A = \mathrm{Softmax}\left(\frac{QK^\top}{\sqrt{d_{\mathrm{emb}}}}\right) \in \mathbb{R}^{L'\times L'}, \tag{3.4}$$

where $\mathrm{Softmax}(\cdot)$ is applied row-wise. Because each row of $A = (a_{ij})_{ij}$ is a probability vector, we define the mean sparsity S by the Shannon entropy:

$$S = -\frac{1}{L'} \sum_{i,j=1}^{L'} a_{ij} \log a_{ij}. \tag{3.5}$$

We compute S for models trained on both the forward (learning-friendly) and reverse (learning-unfriendly) orders of the order-sensitive tasks (Section 5.1). Table 1 shows that the forward order consistently yields lower S, and—since a smaller S directly means higher sparsity—this confirms that learning-friendly orders produce sparser attention. Representative heat maps are provided in Appendix A.

Table 1. Attention sparsity S across target orders. A smaller value of S indicates greater sparsity.

Task	**Target length**	**Sparsity**	
		Forward	**Reverse**
ReLU	$L = 20$	**1.160**	1.640
	$L = 50$	**1.462**	4.319
	$L = 100$	**1.687**	3.195
Square-19	$L = 20$	**1.117**	1.531
	$L = 50$	**1.773**	1.914
	$L = 100$	**1.407**	1.990
Index	$L = 13, d = 2$	**0.848**	2.574
	$L = 13, d = 4$	**0.887**	1.486
	$L = 13, d = 8$	**1.116**	1.596

Because S is derived from the learned attention weights, it is independent of the language-model loss and can serve as an orthogonal diagnostic metric. We also experimented with optimizing permutations under an additional sparsity regularizer that rewards low-entropy attention (cf. Appendix B). Even with this bias, the optimizer failed to discover the learning-friendly order and instead converged to interleaved permutations, suggesting that sparsity alone is insufficient to solve the permutation search in difficult regimes.

4. Proposed Method

We introduce our strategy for discovering a suitable permutation of target token sequences. The key idea is to leverage a characteristic of the training dynamics of deep neural networks: they tend to learn easy samples in the early stages of training, and gradually adapt to harder samples later. This phenomenon has been reported in several contexts in the literature, such as (Arpit et al., 2017) for learning with noisy labels and (Baldock et al., 2021) for identifying difficult examples.

We exploit this property by training a Transformer for a few epochs on a dataset with various orders in mixture and identify learning-friendly orders as "easy samples," for which loss drops faster.

More formally, let $D = \{(X_i, Y_i)\}_{i=1}^{m}$ and $D' = \{(X_i', Y_i')\}_{i=1}^{m'}$ be training and validation sets, respectively. Let $\mathcal{P} = \{P_1, \ldots, P_T\}$ be the set of T candidate permutation matrices. Let D^{P_t} be the set D with reordered target sequences by P_t, i.e., $D^{P_t} = \{(X_i, Y_i P_t)\}_{i=1}^{m}$. We determine learning-friendly orders through the following loss profiling.

P1. Let $E \in \mathbb{N}$. Train a Transformer for E epochs on a mixed dataset $\bar{D} := \bigcup_{t=1}^{T} D^{P_t}$. Let $\mathcal{T}_{\theta'}$ be the Transformer after training.

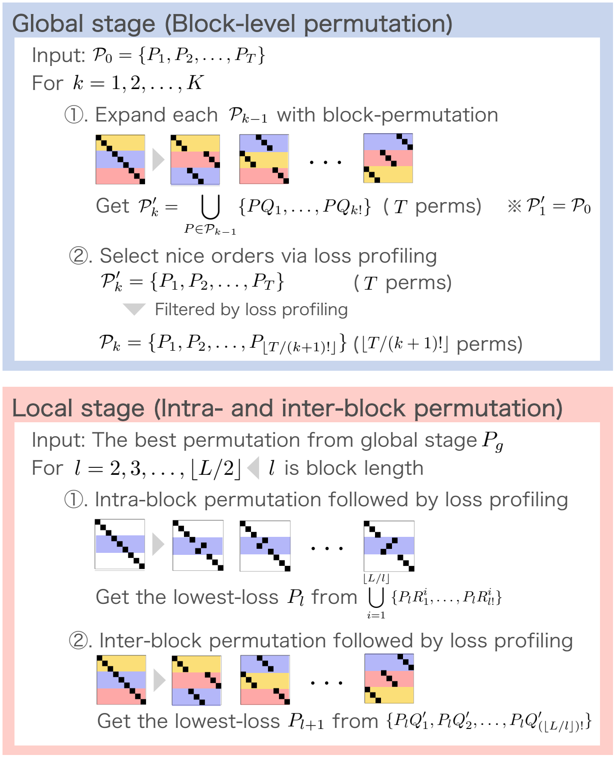
Global stage (Block-level permutation)
Input: $\mathcal{P}_0 = \{P_1, P_2, \ldots, P_T\}$
For $k = 1, 2, \ldots, K$
①. Expand each $\mathcal{P}_{k-1}$ with block-permutation
Get $\mathcal{P}_k' = \bigcup_{P \in \mathcal{P}_{k-1}} \{PQ_1, \ldots, PQ_{k!}\}$ (T perms)
※ $\mathcal{P}_1' = \mathcal{P}_0$
②. Select nice orders via loss profiling
$\mathcal{P}_k' = \{P_1, P_2, \ldots, P_T\}$ (T perms)
Filtered by loss profiling
$\mathcal{P}_k = \{P_1, P_2, \ldots, P_{\lfloor T/(k+1)! \rfloor}\}$ ($\lfloor T/(k+1)! \rfloor$ perms)
Local stage (Intra- and inter-block permutation)
Input: The best permutation from global stage P_g
For $l = 2, 3, \ldots, \lfloor L/2 \rfloor$
l is block length
①. Intra-block permutation followed by loss profiling
Get the lowest-loss P_l from $\bigcup_{i=1}^{\lfloor L/l \rfloor} \{P_l R_1^i, \ldots, P_l R_{l!}^i\}$
②. Inter-block permutation followed by loss profiling
Get the lowest-loss P_{l+1} from $\{P_l Q_1', P_l Q_2', \ldots, P_l Q_{(\lfloor L/l \rfloor)!}'\}$

Figure 3. Search flow of our hierarchical approach. **Global stage**: The proposed method generates T candidate permutations by swapping the sequence at the macro-level, exchanging P token blocks to quickly spot coarse, learning-friendly orders. **Local stage**: inside each chosen block, the proposed method further permutes the tokens, refining the sequence to discover a final permutation that maximises learning ease.

P2. Compute the loss on the validation set D' for each permutation; namely, for $t = 1, \ldots, T$, compute

$$\mathcal{L}(D', P_t) = \frac{1}{m'} \sum_{i=1}^{m'} \ell(\mathcal{T}_{\theta'}, X_i', Y_i' P_t). \tag{4.1}$$

Then, the most learning-friendly order $P^* := P_\tau$ is determined with $\tau = \arg\min_t \mathcal{L}(D', P_t)$.

In our experiments, we empirically observed that a few thousands permutations can be handle at once through this approach. However, the number of permutations grows factorially, which leads us to introduce the following two-stage hierarchical optimization, where aforementioned loss profiling (i.e., **P1** and **P2**) is performed to determine learning-friendly orders at each level.

Figure 3 illustrates our hierarchical method. We start with the initial set of permutation candidates $\mathcal{P}_0 = \{P_1, \ldots, P_T\}$. The global stage splits each token sequence into several blocks and finds a good permutation in block

Table 2. Success rates across different orders in the proposed task. The forward order is learning-friendly, whereas the reverse order is learning-unfriendly.

Task	**Target length**	**Success rate (%)**	
		Forward	**Reverse**
ReLU	$L = 20$	**99.6**	0.6
	$L = 50$	**99.9**	5.6
	$L = 100$	**99.4**	0.0
Square-19	$L = 20$	**100**	0.1
	$L = 50$	**100**	0.0
	$L = 100$	**100**	0.0
Index	$L = 13, d = 2$	**100**	9.8
	$L = 13, d = 4$	**62.3**	1.3
	$L = 13, d = 8$	**81.8**	2.2
	$L = 31, d = 2$	**100**	0.8

level. The local stage refines this coarse ordering by permuting the tokens within each block discovered at the global stage. Formally, the two stages operate as follows.

Global stage. Let the search depth be K and $T = (K + 1)!$. Let $\mathcal{P}_1 := \mathcal{P}_0$, for $k = 1, \ldots, K$, we first (conceptually) split each target sequence into k blocks[1]. We apply the loss profiling to the new permutation set:

$$\bigcup_{P \in \mathcal{P}_k} \{PQ_1, \ldots, PQ_{k!}\}, \tag{4.2}$$

where $Q_i \in [0,1]^{L \times L}$ are the block-level permutations. The best $\lfloor T/(k+1)! \rfloor$ permutations define new candidate set $\mathcal{P}_{k+1}$.

We then apply the loss profiling to the final candidate set $\mathcal{P}_{\mathrm{g}} := \mathcal{P}_{K+1}$ and determine the best permutation P_{g}. This permutation is then refined with the local stage.

Local stage. Let $P_1 := P_{\mathrm{g}}$ is the initial permutation. We again conceptually split each target sequence into blocks of size l. Let $R_1^i, \ldots, R_{l!}^i \in [0,1]^{L \times L}$ be all the permutations inside the i-th block. These permutations do not change the orders outside the i-th block. For each block length $l = \{2, 3, \ldots, \lfloor L/2 \rfloor\}$[2], we apply the loss profiling to new candidate set:

$$\bigcup_{i=1}^{L/l} \{PR_1^i, \ldots, PR_{l!}^i\}, \tag{4.3}$$

and denote the lowest-loss result by P_l. Keeping each block's internal order fixed, we perform loss profiling over the $\lfloor L/l \rfloor$ block-reordering candidates:

$$\{P_l Q'_1,\, P_l Q'_2,\, \ldots,\, P_l Q'_{\lfloor L/l \rfloor}\}. \tag{4.4}$$

The best candidate becomes the initial permutation for the next block size $l + 1$.

With a global-stage depth of K and for a target length L, the hierarchical search visits on the order of $(K + 1)!$ candidate permutations. Empirically, a relatively large batch size 128 examples and just one or two epochs over a training sample of 10^5 pairs suffice, so the entire discovery phase is finished after only a few thousand optimization steps. We also tried evolutionary strategy (cf. Appendix C), but this involves a number of hyper-parameters, and our deterministic approach is more reliable.

5. Experiments

5.1. Order-sensitive tasks

To evaluate the proposed method, we introduce three tasks. They can be learned relatively easily with the forward order, which however becomes challenging with the reverse or random orders.

Let $X = [x_1, x_2, ...]$ be an input sequence and $Y = [y_1, ..., y_L]$ an target sequence of fixed length L. In high level, the target sequence of the three tasks is defined by the following recurrence.

$$y_i = f(X, y_1, ..., y_{i-1}). \tag{5.1}$$

Because $f(\,\cdot\,)$ is *non-injective* in its dependence on the preceding targets, a later value y_i does not uniquely determine its predecessor y_{i-1}. Consequently, any disruption of the natural left-to-right order—such as reversing or randomly permuting the targets—breaks the causal chain and substantially increases the learning difficulty.

ReLU. Here the recurrence performs a running rectified sum: $y_1 = x_1$ and for $i = 2, \ldots, L$,

$$y_i = \mathrm{ReLU}\big(x_i + y_{i-1}\big), \tag{5.2}$$

where $\mathrm{ReLU}(z) = \max(z, 0)$. The forward order is trivial to learn because each step depends only on the current input token x_i and the immediately preceding output y_{i-1}; in the reverse order that dependency becomes latent.

Square-19. The second task accumulates squared values modulo a small prime: $y_1 = x_1$ and for $i = 2, \ldots, L$,

$$y_i = x_i^2 + y_{i-1}^2 \mod 19 \in \{-9, \ldots, 9\}. \tag{5.3}$$

The squaring operation is non-injective: the mapping is many-to-one. Within the interval $z \in [-9, 9]$, the equation $z^2 = 4$ is satisfied by both $z = 2$ and $z = -2$, so the preimage of 4 is not unique.

[1]When $k = 1$, the sequence not split into blocks

[2]If L/l is not an integer, the remaining $L \mod l$ tokens are placed in an additional block.

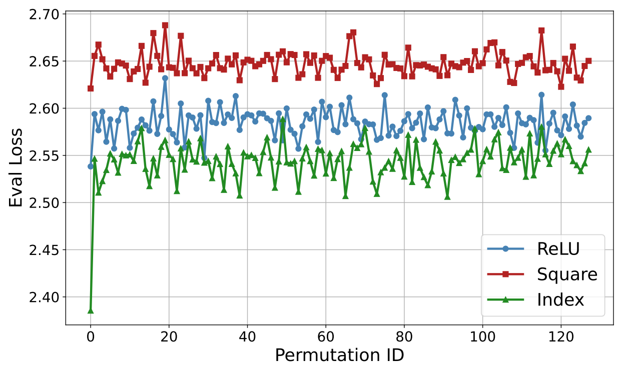

Figure 4. For $\mathcal{P}_g$, the evaluation loss of every permutation is computed after training on the three tasks. Permutation ID 0 corresponds to the forward order, whereas the remaining 127 IDs correspond to randomly generated permutations. The target length is fixed at $L = 13$ for all tasks.

INDEX. The last task uses the recent output history as a pointer into the input: $y_1 = x_1$ and for $i = 2, \dots, L$,

$$y_i = x_p, \quad p = \sum_{j=1}^{d} y_{i-j} \mod L,$$

where $d \leq L$ is a fixed window size. Forward order enables the model to compute p incrementally, whereas a reversed or random order destroys the causal chain.

PROD. Unlike the three tasks proposed above, multiplication has been examined in earlier studies; although it does not satisfy the recurrence in Equation (5.1), it still exhibits a moderate degree of order sensitivity. Given two zero-padded input numbers a and b, the target sequence is their product $Y = [ab]$. When the digits are emitted from least significant to most significant, we denote the sequence by Y (forward order); when the digits are emitted in the opposite direction, we denote it by Y^r (reverse order).

Example 5.1 (SQUARE-19 task)**.** Given the input sequence $X = [7, -2, 4, 1, 3]$ and the initial value $y_1 = x_1 = 7$, applying the recurrence in (5.3) produces

$$\begin{aligned} y_1 &= 7, \\ y_2 &= (-2)^2 + 7^2 \bmod 19 = -4, \\ y_3 &= 4^2 + (-4)^2 \bmod 19 = -6, \\ y_4 &= 1^2 + (-6)^2 \bmod 19 = -1, \\ y_5 &= 3^2 + (-1)^2 \bmod 19 = -9. \end{aligned}$$

In forward order, memorizing just $19^2 = 361$ cases suffices to output the target sequence. In reverse order Y^r , however, even with $y_5 = -9$ known, y_4 is still ambiguous between 1 and -1, so learning becomes much harder. Generation examples for the remaining tasks are provided in Appendix D.

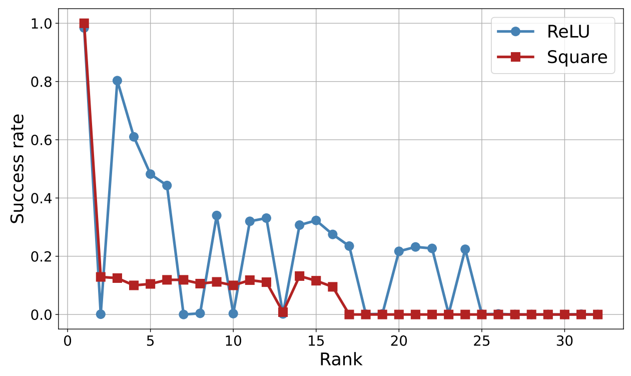

Figure 5. Success rate achieved when the Transformer is retrained on each permutation dataset, ranked for the RELU and SQUARE-19 tasks with $\mathcal{P}_f$.The x-axis lists permutations from highest to lowest rank (left to right). The target length is fixed at $L = 20$.

5.2. Training setup

Training parameters. We use a GPT-2 model (Radford et al., 2019) with six layers and a single attention head. The embedding and feed-forward dimensions are $(d_{\text{emb}}, d_{\text{ffn}}) = (512, 2048)$, and dropout is set to 0.1. Positional embeddings are randomly initialized and remain trainable throughout training. The model is trained for 10 epochs with AdamW (Loshchilov & Hutter, 2019) ($\beta_1 = 0.9, \beta_2 = 0.999$), a linearly decaying learning rate starting from 5.0×10^{-5} , and a batch size of 128.

Dataset. The generation procedure is detailed in Section 5.1. For every task, the target length L is sampled from the range $\{5, 6, \dots, 100\}$. Only the INDEX task introduces a window size d, which is set to $d \in \{2, 4, 8\}$. The training set contains 100,000 samples, and the evaluation set contains 1,000 samples. Different random seeds (42 for training and 123 for evaluation) are used to keep the two sets disjoint.

To reorder them, we consider four permutation sets for $\mathcal{P}$:

- $\mathcal{P}_f$ is obtained by splitting the forward and reverse orders into column-wise blocks and swapping those blocks.
- $\mathcal{P}_r$ denotes a permutation set chosen uniformly at random.
- $\mathcal{P}_g$ contains the forward permutation plus random permutations. For example, if the set size is 100, it includes one forward permutation and 99 random ones.
- $\mathcal{P}_b$ is obtained by splitting the forward and reverse sequence into length b and permutes those blocks, and fix $b = 5$ in experiments.

Table 3. The orders discovered by the proposed method in its global and local stages. Depth denotes the hierarchy level K reached in the global stage. Each order is listed relative to the forward sequence; when the list starts at 0, the forward order has been recovered. Forward orders identified at a given stage are highlighted in bold.

Task	Target Length	Depth	Order after global stage	Discovered final order
ReLU	$L = 7$	$K = 4$	$[6, 0, 5, 2, 3, 4, 1]$	$[2, 3, 4, 5, 0, 6, 1]$
	$L = 8$	$K = 4$	$[0, 2, 1, 3, 4, 5, 6, 7]$	$[\mathbf{0}, \mathbf{1}, \mathbf{2}, \mathbf{3}, \mathbf{4}, \mathbf{5}, \mathbf{6}, \mathbf{7}]$
	$L = 9$	$K = 5$	$[\mathbf{0}, \mathbf{1}, \mathbf{2}, \mathbf{3}, \mathbf{4}, \mathbf{5}, \mathbf{6}, \mathbf{7}, \mathbf{8}]$	$[\mathbf{0}, \mathbf{1}, \mathbf{2}, \mathbf{3}, \mathbf{4}, \mathbf{5}, \mathbf{6}, \mathbf{7}, \mathbf{8}]$
	$L = 10$	$K = 6$	$[6, 7, 8, 9, 5, 4, 2, 3, 1, 0]$	$[4, 5, 6, 7, 8, 9, 0, 1, 2, 3]$
	$L = 11$	$K = 6$	$[8, 9, 10, 7, 6, 5, 4, 3, 2, 1, 0]$	$[\mathbf{0}, \mathbf{1}, \mathbf{2}, \mathbf{3}, \mathbf{4}, \mathbf{5}, \mathbf{6}, \mathbf{7}, \mathbf{8}, \mathbf{9}, \mathbf{10}]$
	$L = 12$	$K = 6$	$[6, 7, 8, 9, 10, 11, 5, 4, 2, 3, 1, 0]$	$[1, 2, 3, 4, 0, 5, 6, 7, 8, 9, 10, 11]$
	$L = 13$	$K = 6$	$[11, 12, 10, 9, 8, 7, 6, 5, 4, 2, 3, 1, 0]$	$[\mathbf{0}, \mathbf{1}, \mathbf{2}, \mathbf{3}, \mathbf{4}, \mathbf{5}, \mathbf{6}, \mathbf{7}, \mathbf{8}, \mathbf{9}, \mathbf{10}, \mathbf{11}, \mathbf{12}]$
Square-19	$L = 7$	$K = 4$	$[\mathbf{0}, \mathbf{1}, \mathbf{2}, \mathbf{3}, \mathbf{4}, \mathbf{5}, \mathbf{6}]$	$[\mathbf{0}, \mathbf{1}, \mathbf{2}, \mathbf{3}, \mathbf{4}, \mathbf{5}, \mathbf{6}]$
	$L = 8$	$K = 4$	$[1, 2, 4, 5, 0, 6, 7, 3]$	$[1, 2, 4, 5, 0, 6, 7, 3]$
	$L = 9$	$K = 5$	$[\mathbf{0}, \mathbf{1}, \mathbf{2}, \mathbf{3}, \mathbf{4}, \mathbf{5}, \mathbf{6}, \mathbf{7}, \mathbf{8}]$	$[\mathbf{0}, \mathbf{1}, \mathbf{2}, \mathbf{3}, \mathbf{4}, \mathbf{5}, \mathbf{6}, \mathbf{7}, \mathbf{8}]$
	$L = 10$	$K = 6$	$[9, 8, 7, 6, 5, 4, 3, 2, 1, 0]$	$[\mathbf{0}, \mathbf{1}, \mathbf{2}, \mathbf{3}, \mathbf{4}, \mathbf{5}, \mathbf{6}, \mathbf{7}, \mathbf{8}, \mathbf{9}]$
	$L = 11$	$K = 6$	$[\mathbf{0}, \mathbf{1}, \mathbf{2}, \mathbf{3}, \mathbf{4}, \mathbf{5}, \mathbf{6}, \mathbf{7}, \mathbf{8}, \mathbf{9}, \mathbf{10}]$	$[\mathbf{0}, \mathbf{1}, \mathbf{2}, \mathbf{3}, \mathbf{4}, \mathbf{5}, \mathbf{6}, \mathbf{7}, \mathbf{8}, \mathbf{9}, \mathbf{10}]$
	$L = 12$	$K = 6$	$[1, 2, 3, 4, 5, 6, 7, 11, 10, 9, 0, 8]$	$[\mathbf{0}, \mathbf{1}, \mathbf{2}, \mathbf{3}, \mathbf{4}, \mathbf{5}, \mathbf{6}, \mathbf{7}, \mathbf{8}, \mathbf{9}, \mathbf{10}, \mathbf{11}]$
	$L = 13$	$K = 6$	$[0, 1, 2, 3, 12, 11, 10, 4, 5, 6, 7, 8, 9]$	$[8, 9, 0, 1, 2, 3, 4, 10, 11, 12, 5, 6, 7]$
Index	$L = 13, d = 2$	$K = 6$	$[1, 0, 2, 3, 4, 5, 6, 7, 8, 9, 10, 11, 12]$	$[\mathbf{0}, \mathbf{1}, \mathbf{2}, \mathbf{3}, \mathbf{4}, \mathbf{5}, \mathbf{6}, \mathbf{7}, \mathbf{8}, \mathbf{9}, \mathbf{10}, \mathbf{11}, \mathbf{12}]$
	$L = 13, d = 4$	$K = 6$	$[0, 1, 7, 6, 4, 2, 5, 8, 3, 9, 10, 11, 12]$	$[0, 1, 7, 6, 4, 2, 5, 8, 3, 9, 10, 11, 12]$
	$L = 13, d = 8$	$K = 6$	$[1, 2, 3, 4, 5, 6, 7, 8, 10, 9, 12, 0, 11]$	$[1, 2, 3, 4, 5, 6, 7, 8, 10, 9, 12, 0, 11]$
Prod	$L = 10$	$K = 6$	$[\mathbf{0}, \mathbf{1}, \mathbf{2}, \mathbf{3}, \mathbf{4}, \mathbf{5}, \mathbf{6}, \mathbf{7}, \mathbf{8}, \mathbf{9}]$	$[\mathbf{0}, \mathbf{1}, \mathbf{2}, \mathbf{3}, \mathbf{4}, \mathbf{5}, \mathbf{6}, \mathbf{7}, \mathbf{8}, \mathbf{9}]$

Examples of these permutation sets are provided in Appendix E.

5.3. Success rate for each order

Table 2 reports the success rate for each task under the forward and reverse output orders. The success rate is defined as the fraction of evaluation samples for which the trained model's output exactly matches the target sequence. As explained in Section 5.1, every task is configured to be learning-friendly in the forward order but learning-unfriendly in the reverse order. Consistent with this design, Table 2 shows that the model almost fully learns each task in the forward order, whereas in the reverse order, the success rate never exceeds roughly 10 %. A closer look at task-specific trends reveals that the success rate for the ReLU and Square-19 tasks remains almost unchanged as the target length grows. By contrast, for Index, the forward order success rate declines with the window size d, indicating that the model struggles when each prediction depends on a larger number of previous outputs.

5.4. Transformer trained with multiple orders

We trained a Transformer on a set of permutations, $\mathcal{P}_{\mathrm{g}}$, containing one learning-friendly forward order (ID 0) and 127 randomly generated learning-unfriendly orders. The evaluation loss for each permutation is plotted in Figure 4, which shows that only the learning-friendly order achieves the lowest loss across all tasks. This indicates that the model preferentially adapts to the learning-friendly sequence when trained on a mixture of orders. This effect is particularly pronounced in the Index task, where the loss for the forward order drops much more steeply than for any other, highlighting a strong preference for this sequence.

Figure 5 reports the success rate obtained when the Transformer is retrained with the permutation ranking produced for the ReLU and Square-19 tasks using $\mathcal{P}_{\mathrm{f}}$. For both tasks, the success rate declines progressively as the ranking position worsens, indicating that our evaluation-loss criterion indeed uncovers orders the model learns most easily. In the Square-19 task, the success rate drops monotonically from left to right—except at rank 13—showing that the ranking is highly accurate.

5.5. Results of the hierarchical search

We perform hierarchical search from two initial permutation-sets. The first, $\mathcal{P}_{\mathrm{r}}$, contains fully random permutations and therefore defines the most challenging setting. The second, $\mathcal{P}_{\mathrm{b}}$, is block-restricted: in many routine mathematical problems—polynomial manipulation is a typical example—only a handful of monomial orders are considered plausible within each block, so the effective search space is far smaller than in the random case. Figure 6 contrasts the

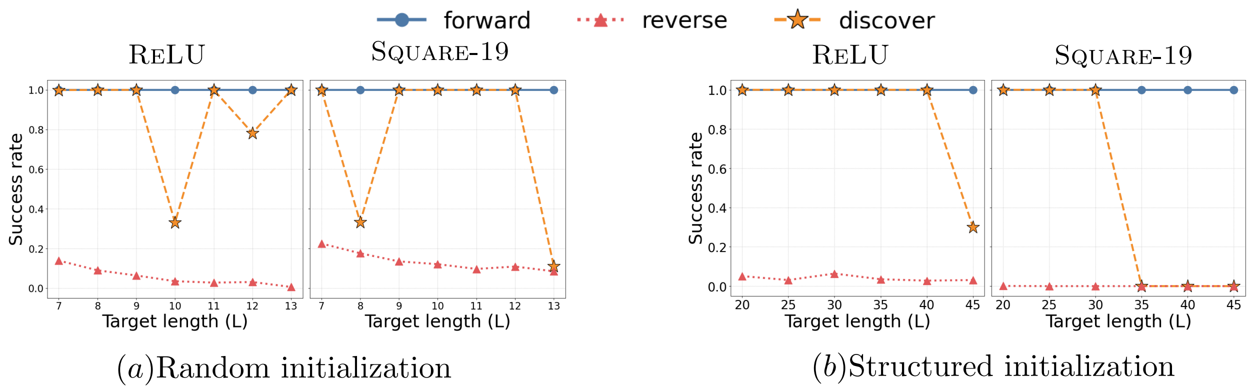

Figure 6. Success rates for the ReLU task at varying target-sequence lengths; (b) corresponding results for the Square-19 task. In each panel, blue represents the learning-friendly forward order, red the learning-unfriendly reverse order, and green the order discovered by our proposed method.

results obtained from these two starting points.

Random search-space initialization. Table 3 lists the permutations discovered by the proposed method when it begins from $\mathcal{P}_{\mathrm{r}}$. After the global stage, tokens that are neighbours in the input usually remain adjacent, showing that the method first captures coarse structure. The subsequent local stage then fine-tunes this order and moves the order closer to the optimal forward arrangement. For the ReLU and Square-19 tasks global order is often already learning-friendly, and retraining a model on the discovered order always produces a higher success rate than training on the reverse order (see Figure 6(a)). The Index task proves harder: as the reference width d grows, learning is difficult even in the forward order (see Section 5.1), which flattens the loss landscape and makes good permutations harder to rank. In the Prod, the proposed method succeeds in rediscovering the least-significant-digit first order reported by (Shen et al., 2023), and it finds the optimal order for target lengths up to 13, identifying a single solution among roughly 6×10^9 possibilities.

Structured search-space initialization. When the search is initialized with $\mathcal{P}_{\mathrm{b}}$, the proposed method scales to much longer target sequences. Figure 6(b) shows the resulting success rate curves for ReLU and Square-19: the optimal order is found for both tasks up to $L = 30$, and for ReLU even at $L = 40$. At $L = 40$ the theoretical permutation space still contains about 10^{47} elements, indicating that once implausible candidates are pruned, the proposed method can explore the remaining space far more effectively. Taken together, these results demonstrate that our hierarchical search is capable of recovering optimal orders in both the most challenging fully random scenario and the more realistic, block-restricted setting, and that its advantage grows as the candidate space is made more coherent.

6. Conclusions

This study addressed a new task of reordering decoder input tokens for Transformers in learning arithmetic tasks. In essence, the proposed method performs short-term training on a mixture of target sequences in different orders and discovers easy samples for which loss drops faster, as learning-friendly orders. To search the factorially large space efficiently, we propose a two-stage hierarchical approach combining global block-level exploration with local refinement. The experiments on three order-sensitive arithmetic tasks (ReLU, Square-19, and Index) demonstrated that the proposed method discovers a learning-friendly order, improving the success rate from about 10 % to near 100 % and works for target lengths up to 13 tokens ($13! > 6 \times 10^9$ permutations). Moreover, it rediscovered the reverse-digit order reported in earlier work on the Prod task. This study presents an automatically unraveling chain of thought that markedly enhances a Transformer's reasoning ability. The extension to longer sequences and target sequences at a variable length will be future work.

Acknowledgments

This research was partially supported by JST PRESTO Grant Number JPMJPR24K4, Mitsubishi Electric Information Technology R&D Center, the Chiba University IAAR Research Support Program and the Program for Forming Japan's Peak Research Universities (J-PEAKS), and JSPS KAKENHI Grant Number JP23K24914.

References

Alfarano, A., Charton, F., and Hayat, A. Global lyapunov functions: a long-standing open problem in mathematics, with symbolic transformers. In *Advances in Neural Information Processing Systems*, 2024.

Arpit, D., Jastrzundefinedbski, S., Ballas, N., Krueger, D., Bengio, E., Kanwal, M. S., Maharaj, T., Fischer, A., Courville, A., Bengio, Y., and Lacoste-Julien, S. A closer look at memorization in deep networks. In *International Conference on Machine Learning*, 2017.

Baldock, R. J. N., Maennel, H., and Neyshabur, B. Deep learning through the lens of example difficulty. In *Advances in Neural Information Processing Systems*, 2021.

Charton, F. Linear algebra with transformers. *Transactions on Machine Learning Research*, 2022.

Chen, W., Ma, X., Wang, X., and Cohen, W. W. Program of thoughts prompting: Disentangling computation from reasoning for numerical reasoning tasks. *Transactions on Machine Learning Research*, 2023.

Forouzesh, M. and Thiran, P. Differences between hard and noisy-labeled samples: An empirical study. In *Proceedings of the 2024 SIAM International Conference on Data Mining (SDM)*, pp. 91–99, 2024.

Hahn, M. and Rofin, M. Why are sensitive functions hard for transformers? In *Proceedings of the Annual Meeting of the Association for Computational Linguistics*, 2024.

Han, B., Yao, Q., Yu, X., Niu, G., Xu, M., Hu, W., Tsang, I., and Sugiyama, M. Co-teaching: Robust training of deep neural networks with extremely noisy labels. In *Advances in Neural Information Processing Systems*, 2018.

Jang, E., Gu, S., and Poole, B. Categorical reparameterization with gumbel-softmax. In *International Conference on Learning Representations*, 2017.

Jelassi, S., d'Ascoli, S., Domingo-Enrich, C., Wu, Y., Li, Y., and Charton, F. Length generalization in arithmetic transformers, 2023.

Jiang, L., Zhou, Z., Leung, T., Li, L.-J., and Fei-Fei, L. Mentornet: Learning data-driven curriculum for very deep neural networks on corrupted labels. In *International Conference on Machine Learning*, 2018.

Kera, H., Ishihara, Y., Kambe, Y., Vaccon, T., and Yokoyama, K. Learning to compute gröbner bases. In *Advances in Neural Information Processing Systems*, 2024.

Kera, H., Pelleriti, N., Ishihara, Y., Zimmer, M., and Pokutta, S. Computational algebra with attention: Transformer oracles for border basis algorithms. *arXiv:2505.23696*, 2025.

Kim, J. and Suzuki, T. Transformers provably solve parity efficiently with chain of thought. In *International Conference on Learning Representations*, 2025.

Kojima, T., Gu, S. S., Reid, M., Matsuo, Y., and Iwasawa, Y. Large language models are zero-shot reasoners. In *Advances in Neural Information Processing Systems*, 2022.

Lample, G. and Charton, F. Deep learning for symbolic mathematics. In *International Conference on Learning Representations*, 2020.

Li, C. Y., Sotáková, J., Wenger, E., Malhou, M., Garcelon, E., Charton, F., and Lauter, K. Salsapicante: A machine learning attack on lwe with binary secrets. In *Proceedings of the ACM SIGSAC Conference on Computer and Communications Security*, 2023a.

Li, C. Y., Wenger, E., Allen-Zhu, Z., Charton, F., and Lauter, K. E. Salsa verde: a machine learning attack on learning with errors with sparse small secrets. In *Advances in Neural Information Processing Systems*, 2023b.

Loshchilov, I. and Hutter, F. Decoupled weight decay regularization. In *International Conference on Learning Representations*, 2019.

Mena, G., Belanger, D., Linderman, S., and Snoek, J. Learning latent permutations with gumbel-sinkhorn networks. In *International Conference on Learning Representations*, 2018.

Radford, A., Wu, J., Child, R., Luan, D., Amodei, D., and Sutskever, I. Language models are unsupervised multitask learners. *OpenAI*, 2019.

Rahaman, N., Baratin, A., Arpit, D., Draxler, F., Lin, M., Hamprecht, F., Bengio, Y., and Courville, A. On the spectral bias of neural networks. In *International Conference on Machine Learning*, 2019.

Shalev-Shwartz, S., Shamir, O., and Shammah, S. Failures of gradient-based deep learning. In *International Conference on Machine Learning*, 2017.

Shen, R., Bubeck, S., Eldan, R., Lee, Y. T., Li, Y., and Zhang, Y. Positional description matters for transformers arithmetic. *arXiv:2311.14737*, 2023.

Swayamdipta, S., Schwartz, R., Lourie, N., Wang, Y., Hajishirzi, H., Smith, N. A., and Choi, Y. Dataset cartography: Mapping and diagnosing datasets with training dynamics. In *Proceedings of EMNLP*, 2020.

Vaswani, A., Shazeer, N., Parmar, N., Uszkoreit, J., Jones, L., Gomez, A. N., Kaiser, L., and Polosukhin, I. Attention is all you need. In *Advances in Neural Information Processing Systems*, 2017.

Wei, J., Wang, X., Schuurmans, D., Bosma, M., Ichter, B., Xia, F., Chi, E., Le, Q., and Zhou, D. Chain-of-thought prompting elicits reasoning in large language models. In *Advances in Neural Information Processing Systems*, 2022.

Wenger, E., Chen, M., Charton, F., and Lauter, K. E. SALSA: attacking lattice cryptography with transformers. In *Advances in Neural Information Processing Systems*, 2022.

Yao, S., Yu, D., Zhao, J., Shafran, I., Griffiths, T. L., Cao, Y., and Narasimhan, K. Tree of thoughts: Deliberate problem solving with large language models. In *Advances in Neural Information Processing Systems*, 2023.

Zhang, C., Bengio, S., Hardt, M., Recht, B., and Vinyals, O. Understanding deep learning requires rethinking generalization. In *International Conference on Learning Representations*, 2017.

Zhang, X., Du, C., Pang, T., Liu, Q., Gao, W., and Lin, M. Chain of preference optimization: Improving chain-of-thought reasoning in LLMs. In *Advances in Neural Information Processing Systems*, 2024.

A. Visualizing attention map

We present the attention maps obtained when training a Transformer on our proposed ReLU task with datasets reordered in different ways. For this analysis, we use a GPT-2 model with a single layer and a single attention head. Figure 7 shows the attention maps for target length $L = 20$ under four target orders. The forward and reverse orders are defined in Section 5.1. The one-permuted order swaps exactly one pair of adjacent target tokens, whereas the random order is a random permutation of the forward sequence. Figure 8 illustrates how the attention maps change as the target length increases.

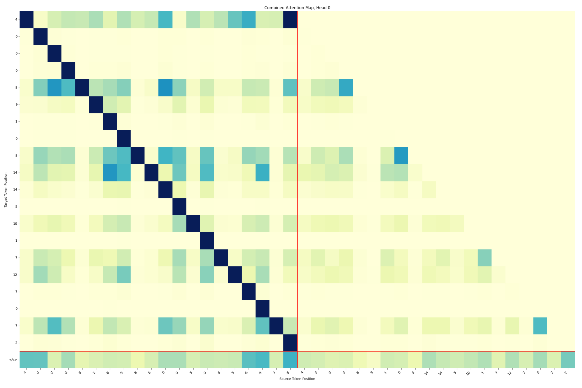

(a) Forward order

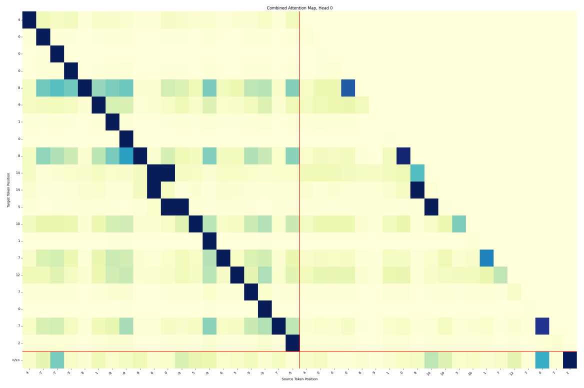

(b) one permuted order

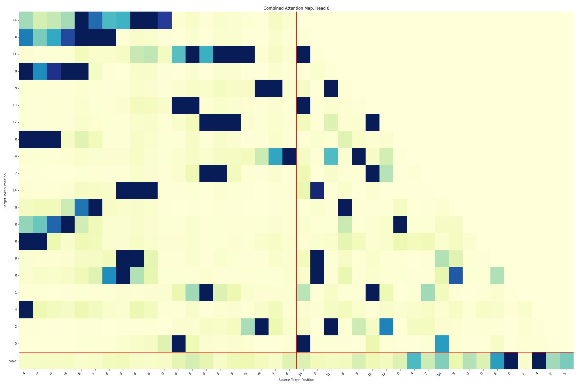

(c) Random order

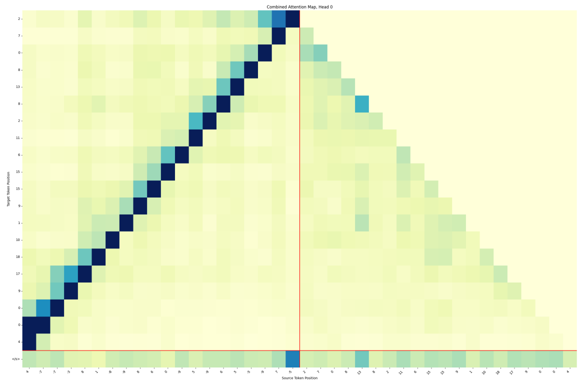

(d) Reverse order

Figure 7. Attention matrices from models trained with four different target orders in the ReLU task.

B. Soft-permutation optimization via attention sparsity

In this section, we present a soft-permutation optimization method based on attention sparsity. In our two-stage strategy, we first optimize the Transformer parameters θ by minimizing the standard sequence-modeling loss over the training set:

$$\min_{\theta} \frac{1}{m} \sum_{i=1}^{m} \ell\big(\mathcal{T}_\theta, X_i, Y_i\big). \tag{B.1}$$

Next, denoting by $A = [a_{ij}] \in \mathbb{R}^{L' \times L'}$ the attention map produced when the target sequence is fed as $Y_i \tilde{P}$ into the Transformer, we optimize the soft permutation $\tilde{P}$ by minimizing the total attention entropy:

$$\min_{\tilde{P}} \frac{1}{L'} \sum_{i=1}^{L'} \sum_{j=1}^{L'} a_{ij}. \tag{B.2}$$

In the experiments, we alternate between the two-stage optimizations at each step. Figure 9 compares the stage 2 loss

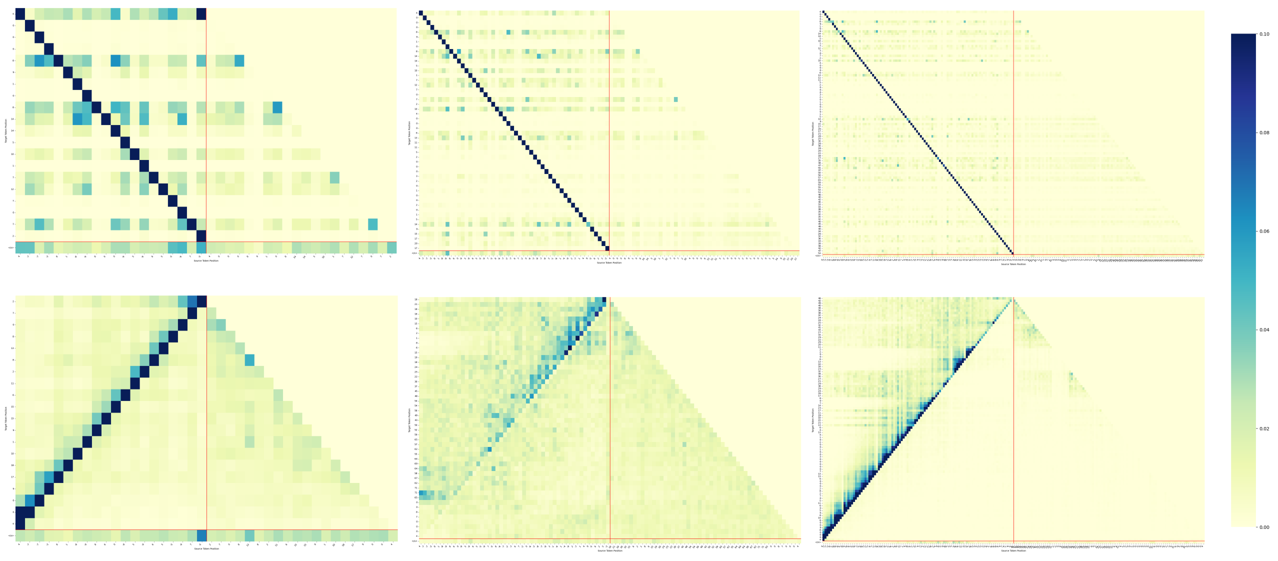

Figure 8. Differences in the attention matrices for the ReLU task between forward and reverse orderings. The top three matrices correspond to models trained with forward order, and the bottom three with reverse order. Each pair of matrices shows results for input lengths $n = 20$, 50, and 100, respectively.

under three conditions: the fixed, learning-friendly order, the fixed, learning-unfriendly (reverse) order, and the learned soft permutation. We observe that the soft permutation does not reduce the entropy-based loss (B.2) relative to the fixed orders, nor does it yield a genuinely hard ordering. Because attention sparsity—as measured by total attention mass—decreases even for static orders, it cannot serve as a reliable objective for permutation optimization.

C. Permutation search via evolutionary strategy

This section summarizes the evolutionary strategy (ES) baseline that we ran in parallel with our proposed method to search the permutation space. Each individual is a permutation P; its fitness is the (negative) early-stage training loss of a Transformer trained with that order, so that permutations that are easier to learn receive higher scores. The ES is controlled by the population size N_p, crossover probability N_c, mutation probability N_m, number of generations N_g, tournament size N_t, and elitism ratio N_r, and proceeds as follows:

(1) **Population initialization:** sample N_p random permutations.

(2) **Selection:** pick parents via tournament selection with size N_t.

(3) **Crossover:** with probability N_c, apply partially–mapped crossover to each selected pair.

(4) **Mutation:** with probability N_m, swap two positions in the offspring permutation.

(5) **Elitism:** evaluate every individual by

$$\text{fitness}(P) = -\frac{1}{m'} \sum_{i=1}^{m'} \ell\big(\mathcal{T}_\theta,\, X_i,\, Y_i P\big),$$

and copy the top N_r fraction to the next generation.

(6) **Termination:** stop when N_g generations have been processed.

Table 4 lists the permutation identified by the evolution strategy (ES) and the performance obtained when the model is retrained using that order.

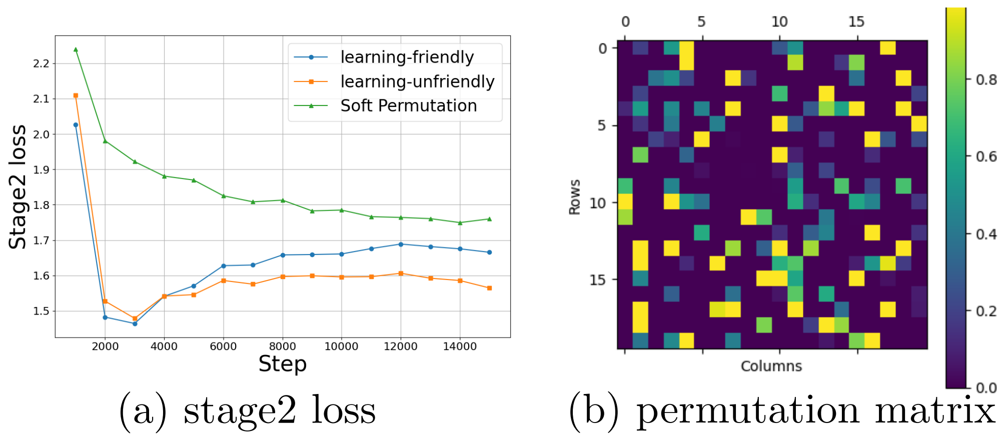

Figure 9. (a) Comparison of Stage 2 loss under fixed learning-friendly order, fixed learning-unfriendly order, and learned soft permutation. (b) shows a visualization of the learned soft permutation.

Table 4. Success rate obtained when the Transformer is retrained on the permutations discovered by the ES.

Task	**Input length**	**ES-discovered order**	**Success rate (%)**	
			Retrain	**Reverse**
ReLU	$L = 5$	$[2, 1, 0, 4, 3]$	26.9	10.4
	$L = 10$	$[0, 1, 2, 3, 4, 5, 6, 7, 8, 9]$	100	3.5
	$L = 20$	$[6, 7, 9, 8, 12, 11, 13, 18, 17, 14, 16, 15, 19, 5, 10, 1, 0, 3, 4, 2]$	9.2	0.7
Square-M19	$L = 5$	$[1, 2, 3, 4, 0]$	100	21.5
	$L = 10$	$[3, 4, 5, 6, 7, 8, 9, 1, 0, 2]$	99.9	13.5
	$L = 20$	$[9, 10, 11, 12, 13, 14, 2, 3, 4, 5, 6, 15, 16, 17, 18, 19, 0, 1, 7, 8]$	5.2	1.2
Index $(m = 2)$	$L = 13$	$[0, 1, 2, 3, 4, 10, 9, 5, 6, 12, 11, 7, 8]$	27.6	7.8

D. Example dataset

This section provides concrete examples for the four tasks introduced in Section 5.1. Table 5 summarizes the correspondence between the input X and the target Y, with every Y given in the forward—that is, learning-friendly—order. For the Prod task only, the input consists of two integers, a and b.

E. Example set of permutations

This section describes the four permutation sets introduced in Section 5.2. Figure 10 visualizes every permutation P in those four sets. Each set contains 32 elements.

Table 5. Representative input–output samples for each task

Task	Input	Target
ReLU, $L = 50$	$X = (4,\ -7,\ -7,\ -3,\ 8,\ 1,\ -8,\ -9,\ 8,\ 6$ $0,\ -9,\ 5,\ -9,\ 6,\ 5,\ -5,\ -9,\ 7,\ -5$ $8,\ -6,\ -7,\ -2,\ -7,\ 6,\ 7,\ -2,\ 0,\ -6$ $-3,\ -8,\ -7,\ -8,\ 3,\ -1,\ -6,\ 1,\ -4,\ -9$ $2,\ -7,\ 1,\ 4,\ 9,\ -5,\ 6,\ 2,\ 3,\ -3)$	$Y = (4,\ 0,\ 0,\ 0,\ 8,\ 9,\ 1,\ 0,\ 8,\ 14$ $14,\ 5,\ 10,\ 1,\ 7,\ 12,\ 7,\ 0,\ 7,\ 2$ $10,\ 4,\ 0,\ 0,\ 0,\ 6,\ 13,\ 11,\ 11,\ 5$ $2,\ 0,\ 0,\ 0,\ 3,\ 2,\ 0,\ 1,\ 0,\ 0$ $2,\ 0,\ 1,\ 5,\ 14,\ 9,\ 15,\ 17,\ 20,\ 17)$
Square-M19, $L = 50$	$X = (-5,\ -9,\ 8,\ 7,\ 8,\ -7,\ 5,\ -9,\ -6,\ 9$ $-2,\ -8,\ 6,\ -7,\ 2,\ -7,\ -6,\ -5,\ -5,\ 7$ $3,\ 6,\ -9,\ 1,\ 7,\ 0,\ -7,\ 7,\ -5,\ 0$ $-2,\ 6,\ -1,\ -9,\ -6,\ -7,\ 0,\ 2,\ 7,\ -1$ $1,\ -2,\ -6,\ -7,\ 5,\ 1,\ 9,\ -6,\ -3,\ -3)$	$Y = (-5,\ 2,\ 2,\ 6,\ -4,\ -1,\ -2,\ 0,\ 8,\ 3$ $4,\ -5,\ -5,\ 8,\ 2,\ 6,\ 6,\ -5,\ 3,\ -8$ $7,\ 0,\ -4,\ 8,\ 9,\ -4,\ -1,\ 3,\ 6,\ 8$ $2,\ -7,\ 3,\ 5,\ -5,\ 8,\ -2,\ -1,\ 3,\ 1$ $-7,\ 6,\ 6,\ 0,\ -3,\ 1,\ -3,\ -2,\ 4,\ -3)$
Index, $L = 13, d = 2$	$X = (1,\ 5,\ 12,\ 3,\ 8,$ $6,\ 11,\ 12,\ 2,\ 8,\ 10,\ 8,\ 10)$	$Y = (5,\ 6,\ 8,\ 5,\ 1,\ 11,$ $10,\ 2,\ 10,\ 10,\ 12,\ 8,\ 12)$
Index, $L = 13, d = 4$	$X = (1,\ 5,\ 12,\ 3,\ 8,$ $6,\ 11,\ 12,\ 2,\ 8,\ 10,\ 8,\ 10)$	$Y = (5,\ 6,\ 8,\ 5,\ 1,\ 11,$ $10,\ 2,\ 10,\ 10,\ 12,\ 8,\ 12)$
Index, $L = 13, d = 8$	$X = (1,\ 5,\ 12,\ 3,\ 8,$ $6,\ 11,\ 12,\ 2,\ 8,\ 10,\ 8,\ 10)$	$Y = (5,\ 6,\ 8,\ 5,\ 1,\ 11,$ $10,\ 2,\ 10,\ 10,\ 12,\ 8,\ 12)$
Prod, $L = 10$	$a = (0,\ 0,\ 2,\ 0,\ 3)$ $b = (0,\ 2,\ 6,\ 3,\ 7)$	$Y = (1,\ 1,\ 3,\ 5,\ 3,\ 5,\ 0,\ 0,\ 0,\ 0)$

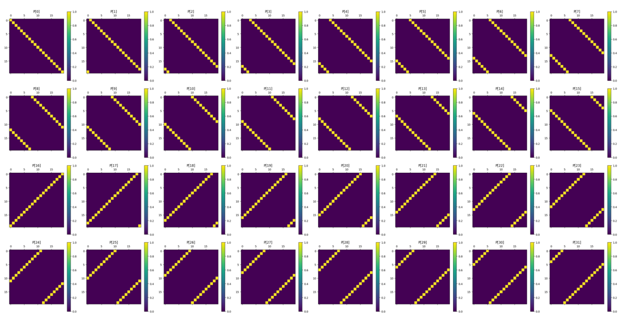
(a) $\mathcal{P}_\mathrm{f}$

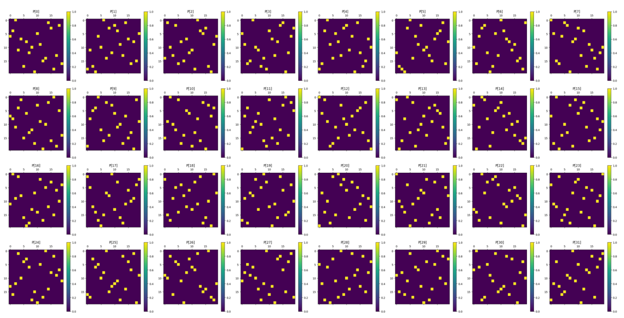
(b) $\mathcal{P}_\mathrm{r}$

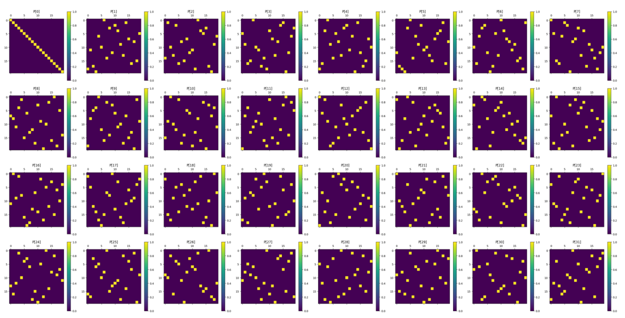
(c) $\mathcal{P}_\mathrm{g}$

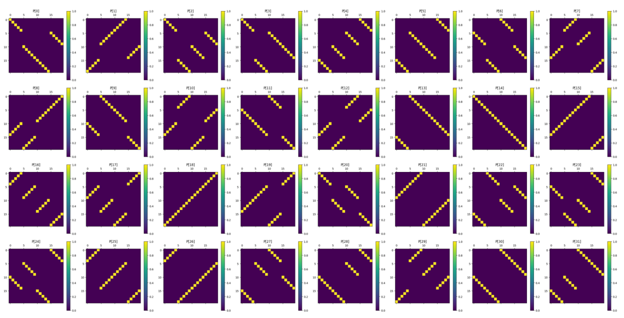
(d) $\mathcal{P}_\mathrm{b}$

Figure 10. Visualization of the elements in the four permutation sets.